8-5-2020

# Neutral, water-soluble poly(ester amide) hydrogels for cell encapsulation

Natalie Liang
*Western University*

Lauren E. Flynn
*Western University*

Elizabeth R. Gillies
*Western University*

# Neutral, water-soluble poly(ester amide) hydrogels for cell encapsulation

Natalie Liang,[a,b] Lauren E. Flynn,[b,c,d*] and Elizabeth R. Gillies[a,b,c*]

[a] Department of Chemistry and the Centre for Advanced Materials and Biomaterials Research, The University of Western Ontario, 1151 Richmond St., London, Ontario, Canada, N6A 5B7

[b] Bone and Joint Institute, The University of Western Ontario, The Sandy Kirkley Centre for Musculoskeletal Research, University Hospital B6-200, London, Ontario, Canada, N6G 2V4

[c] Department of Chemical and Biochemical Engineering, The University of Western Ontario, 1151 Richmond St., London, Ontario, Canada, N6A 5B9

[d] Department of Anatomy and Cell Biology, The University of Western Ontario, 1151 Richmond St., London, Ontario, Canada, N6A 3K7

*authors to whom correspondence should be addressed: lauren.flynn@uwo.ca, egillie@uwo.ca

**Abstract**

Hydrogels are of significant interest for cell encapsulation and delivery in regenerative medicine. Poly(ester amide)s (PEAs) are a class of biodegradable polymers that exhibit promise for biomedical applications due to the degradability of the ester and amide linkages in their backbones, their preparation from biomolecules such as amino acids, and the ability to readily

tune their properties through a modular synthesis approach. Water-soluble PEAs containing cationic arginine moieties have previously been developed, but to the best of our knowledge, neutral water-soluble PEAs based on non-charged amino acids have not been reported. Using a poly(ethylene glycol) (PEG)-based macromonomer, we described here the syntheses of water-soluble amino acid-containing PEAs containing crosslinkable alkenes in their backbones. These PEAs were converted into hydrogels through photoinitiated crosslinking and their properties were compared, including gel content, water content, swelling, and Young's moduli. Subsequent cell culture studies on a subset of hydrogels confirmed that human adipose-derived stromal cells (ASCs) showed >75% viability at 24 hours post-encapsulation. To explore the potential of the hydrogels as cell delivery systems for applications in soft tissue regeneration, adipogenic differentiation of the encapsulated ASCs was probed *in vitro* at 7 days. Analysis of glycerol-3-phosphate dehydrogenase (GPDH) enzyme activity and intracellular lipid accumulation indicated that the hydrogels provided a supportive environment for ASC adipogenesis. Overall, these PEAs provide a new platform that warrants further development for regenerative medicine applications.

**Keywords**

Poly(ester amide), hydrogel, regenerative medicine, adipose-derived stromal cell

## Introduction

Hydrogels are commonly used as scaffolds for cell delivery and tissue engineering due to their high water content resembling that of soft tissues and high permeability to oxygen, nutrients and metabolites [1-3]. Biopolymers such as collagen [4], alginate [5], chitosan [6], hyaluronic acid (HA) [7] and chondroitin sulfate [8] have been extensively investigated for the preparation of hydrogels. These materials can be degraded enzymatically, and can have favorable biological

properties, as they are found naturally within or mimic components of the native extracellular matrix (ECM) within human tissues. However, challenges for natural materials include batch-to-batch reproducibility in their isolation and processing, as well as limitations in the extent to which one can tune their chemical and mechanical properties [9]. On the other hand, synthetic materials can offer a high degree of chemical and mechanical tunability. Polymers including poly(ethylene glycol) (PEG) [10, 11], poly(lactic acid) [11, 12], and poly(*N*-isopropylacrylamide) [13] have been widely explored in hydrogel scaffolds for cell culture and delivery, but without functionalization these polymers lack the innate biological cues offered by biopolymers.

Poly(ester amide)s (PEAs) are a class of polymers containing ester and amide linkages in their backbones, which offer advantages of both polyesters and polyamides, including the biodegradability of polyesters and high mechanical strength and thermal stability of polyamides [14, 15]. In particular, PEAs derived from amino acids, diols, and dicarboxylic acids have been investigated for biomedical applications as they offer advantageous aspects of both natural and synthetic polymers. The incorporated amino acids can be recognized by biological systems and their enzymatic biodegradation leads to metabolically-degradable building blocks, while their properties can be readily tuned by varying their monomer components [16-18]. Most of the incorporated amino acids, diols, and dicarboxylic acids are hydrophobic and the backbone esters and amides do not impart water-solubility. Consequently, a vast majority of the investigated amino-acid containing PEAs have been insoluble in aqueous solution and were processed to form particles [19-21], coatings [22-26], or porous scaffolds by electrospinning [27-30] or particulate leaching methods [31-33]. However, water-insoluble PEAs cannot be used to prepare hydrogels capable of encapsulating cells during the gelation process.

Thus far, only a few examples of water-soluble PEAs have been reported. We reported PEA-PEG graft copolymers that self-assembled into micelles with PEA cores and PEG coronas

for drug delivery applications [34-36]. However, this structural design did not allow for crosslinking to form hydrogel networks, as required for cell delivery applications. Chu and coworkers developed cationic water-soluble PEAs based on L-arginine (Arg) [37] and by introducing crosslinkable fumaramide moieties into their backbone, they were able to incorporate these PEAs into hydrogels with poloxamer-diacrylate [38], methacrylate-functionalized HA [39], glycidyl methacrylate chitosan [40], and gelatin [41]. Alternatively, pendent allyl groups could also be incorporated as crosslinkers [42]. While cationic Arg moieties are effective in solubilizing PEAs in water, and can lead to favorable cell attachment in some cases [38], cationic polymers can be toxic at high concentrations [43] and Arg in particular can interact with phospholipids through bidentate hydrogen bonding and electrostatics, potentially leading to membrane disruption or pore formation [44]. To the best of our knowledge, neutral water-soluble PEAs have not yet been reported.

Here, we report the development of the first non-charged water-soluble PEAs with crosslinkable moieties to enable hydrogel formation and cell encapsulation. Water solubility was achieved by the incorporation of a PEG-based macromonomer into the PEA backbone, while crosslinking capabilities were introduced using fumaramides. The amino acid and diol components were varied. Properties including gel content, water content, swelling, and Young's moduli of the hydrogels fabricated from the different PEAs, and those prepared from the PEAs with PEG or chondroitin sulfate crosslinkers were studied. Subsequently *in vitro* culture studies were performed to investigate the potential of the PEA hydrogels as a cell encapsulation platform. Human adipose-derived stromal cells (ASCs) were used in these studies, as they represent an abundant and readily-accessible pro-regenerative cell source [45]. In particular, the delivery of ASCs within hydrogels has shown promise in adipose tissue engineering strategies seeking to restore defects caused by trauma, disease or aging [46, 47]. As such, human ASCs

were encapsulated into the hydrogels through UV crosslinking and their viability and density were assessed at 24 hr post-encapsulation and at 7 days following the induction of adipogenic differentiation in culture. In addition, analysis of glycerol-3-phosphate dehydrogenase (GPDH) activity, a key enzyme involved in lipid biosynthesis, and intracellular lipid accumulation were performed to determine whether the adipogenic differentiation of the encapsulated ASCs was impacted by the composition of the PEAs.

## Materials and Methods

**General Materials.** Monomers **1a** (L-phenylalanine-1,4-butanediol diester) [48], **1b** (L-phenylalanine-1,8-octanediol diester) [48], **1c** (L-alanine-1,8-octanediol diester) [49] and **3** (di-*p*-nitrophenyl fumarate) [48] were synthesized as previously reported. Macromonomer **2** (diamino PEG, 2000 g/mol) and PEG-dimethacrylate (PEG-DMA, 2000 g/mol) were synthesized as described in the supporting information (Schemes S1-S2). Methacrylated chondroitin sulfate (MCS) with 17% methacrylation was prepared as previously reported [50]. PEG diol (2000 g/mol) was purchased from Alfa Aesar (Haverhill, MA, USA). 4-Dimethylaminopyridine (DMAP) and *p*-toluenesulfonyl chloride were purchased from AK Scientific Inc. (Union City, CA, USA). Chondroitin sulfate (50,000 g/mol) was purchased from LKT Laboratories (St. Paul, MN, USA). Toluene, $NH_4OH$, $MgSO_4$, $Et_3N$, $CH_2Cl_2$, and *N,N*-dimethylacetamide (DMA) were purchased from Caledon Laboratories Inc. (Georgetown, Canada). All other chemicals were purchased from Sigma Aldrich (St. Louis, MO, USA). All chemicals were used as received unless otherwise noted. Under a nitrogen atmosphere, toluene was distilled over sodium, while $Et_3N$, $CH_2Cl_2$, and DMA were distilled over $CaH_2$.

**General procedures.** Dialysis was performed using Spectra/Por 6 dialysis tubing from Spectrum Laboratories (Rancho Dominguez, CA, USA) with molecular weight cutoff (MWCO) of 10 kg/mol. $^1$H nuclear magnetic resonance (NMR) spectra were recorded on either a 400 HMz Bruker AvIII HD instrument or a 600 MHz Varian INOVA instrument (Figures S1-S7). Chemical shifts (δ) are reported in parts per million with the residual protonated solvent signals of $CDCl_3$ (δ 7.26), $D_2O$ (δ 4.80) or DMSO-$d_6$ (2.50) as references. Fourier-transform infrared (FT-IR) spectra were obtained using a Perkin Elmer FT-IR Spectrum Two instrument in attenuated total reflectance (ATR) mode (Figure S8). Size exclusion chromatography (SEC) was performed using an instrument equipped with a Waters 515 HPLC pump, a Waters In-Line Degasser AF, two PLgel mixed D 5μm (300 x 1.5 mm) columns connected to a corresponding PLgel guard column, and a Wyatt Optilab Rex RI detector operating at 658 nm (Figure S9). Samples were dissolved in DMF containing 10 mM LiBr and 1% v/v $Et_3N$ at a concentration of ~5 mg/mL. Samples were filtered through 0.22 μm polytetrafluoroethylene (PTFE) syringe filters, and then injected using a 50 μL loop. Samples were run at a flow rate of 1 mL/min for 30 min at 85 °C. The number average molar mass ($M_n$), weight average molar mass ($M_w$), and dispersity ($Đ$) were determined relative to poly(methyl methacrylate) (PMMA) standards.

**Synthesis of Phe-PEA.** Monomer **1a** (0.30 g, 0.42 mmol, 0.30 equiv.), macromonomer **2** (2.0 g, 0.98 mmol, 0.70 equiv.), and monomer **3** (0.50 g, 1.4 mmol, 1.0 equiv.) were dissolved with stirring in dry DMA (8.0 mL) at 60 °C. $Et_3N$ (0.43 mL, 3.1 mmol, 2.2 equiv.) was added dropwise to the solution, and then it was stirred at 70 °C for 6 hr. The resulting solution was concentrated, re-dissolved in $CH_2Cl_2$ and precipitated in cold diethyl ether (250 mL). The crude product was purified by dialysis against DMF (500 mL) for 48 hr. The solution was then

concentrated, re-dissolved in $CH_2Cl_2$ and precipitated in cold diethyl ether (250 mL). The product was centrifuged, the liquid decanted, and then the solid was dried *in vacuo* to yield a white solid. Yield: 70%. $^1$H NMR (400 MHz, DMSO-$d_6$): $\delta$ 8.92-8.87 (m, 0.69H), 8.50-8.46 (m, 1.64H), 7.30-7.19 (m, 4.29H), 6.86-6.83 (m, 2.00H), 4.58-4.52 (m, 0.78H), 3.98 (s, 1.44H), 3.70-3.66 (m, 1.46H), 3.51 (s, 190H) 3.07-2.89 (m, 2.92H) 1.45 (s, 1.48H). FT-IR: 3510, 3295, 2880, 1740, 1640, 1550 cm$^{-1}$. SEC: $M_n$ = 19.9 kg/mol, $M_w$ = 49.2 kg/mol, $Đ$ = 2.46.

**Synthesis of Phe-8-PEA.** Monomer **1b** (0.066 g, 0.084 mmol, 0.30 equiv.), macromonomer **2** (0.40 g, 0.19 mmol, 0.70 equiv.), and monomer **3** (0.10 g, 0.28 mmol, 1.0 equiv.) were dissolved with stirring in dry DMA (2.0 mL) at 60 °C. $Et_3N$ (0.10 mL, 0.61 mmol, 2.2 equiv.) was added dropwise to the solution, and then it was stirred at 70 °C for 6 hr. The resulting solution was concentrated, re-dissolved in $CH_2Cl_2$ and precipitated in cold diethyl ether (100 mL). The crude product was purified by dialysis against DMF (200 mL) for 48 hr. The solution was then concentrated, re-dissolved in $CH_2Cl_2$ and precipitated in cold diethyl ether (100 mL). The product was centrifuged, the liquid decanted, and then the solid was dried *in vacuo* to yield a white solid. Yield: 58%. $^1$H NMR (400 MHz, DMSO-$d_6$): $\delta$ 8.89-8.85 (m, 0.69H), 8.50-8.45 (m, 1.58H), 7.29-7.18 (m, 4.23H), 6.85-6.82 (m, 2.00H), 4.56-4.51 (m, 0.66H), 4.00-3.97 (m, 1.36H), 3.69-3.67 (m, 1.25H), 3.51 (s, 187H), 3.07-2.89 (m, 2.70H), 1.46 (s, 1.49H), 1.19 (s, 3.61H). FT-IR: 3520, 3300, 2880, 1730, 1630, 1550 cm$^{-1}$. SEC: $M_n$ = 20.1 kg/mol, $M_w$ = 56.6 kg/mol, $Đ$ = 2.81.

**Synthesis of Ala-PEA.** Monomer **1c** (0.26 g, 0.42 mmol, 0.30 equiv.), macromonomer **2** (2.0 g, 0.98 mmol, 0.70 equiv.), and monomer **3** (0.50 g, 1.4 mmol, 1.0 equiv.) were dissolved with stirring in dry DMA (8.0 mL) at 60 °C. $Et_3N$ (0.43 mL, 3.1 mmol, 2.2 equiv.) was added

dropwise to the solution, and then it was stirred at 70 °C for 6 hr. The resulting solution was concentrated, re-dissolved in $CH_2Cl_2$ and precipitated in cold diethyl ether (250 mL). The crude product was purified by dialysis against DMF (500 mL) for 48 hr. The solution was then concentrated, re-dissolved in $CH_2Cl_2$ and precipitated in cold diethyl ether (250 mL). The product was centrifuged, the liquid decanted, and then the solid was dried *in vacuo* to yield a white solid. Yield: 77%. $^1$H NMR (400 MHz, DMSO-$d_6$): $\delta$ 8.82-8.78 (m, 0.59H), 8.51-8.45 (m, 1.46H), 6.89-6.83 (m, 2.00H), 4.34-4.29 (m, 0.64H), 4.08-3.97 (m, 1.41H), 3.71-3.65 (m, 1.98H), 3.51 (s, 177H), 1.54 (s, 1.41H), 1.31-1.22 (m, 5.12H). FT-IR: 3521, 3296, 2880, 1737, 1639, 1546 $cm^{-1}$. SEC: $M_n$ = 18.9 kg/mol, $M_w$ = 56.1 kg/mol, $Đ$ = 2.96.

**Fabrication of hydrogels**. Pure (Phe-PEA or Ala-PEA alone) and hybrid (Phe-PEA/Ala-PEA + PEG-DMA/MCS) hydrogels were fabricated without ASCs for physical characterization studies. All hydrogels were made with a polymer solution concentration of 10% (m/v) in PBS. For the hybrid hydrogels, the prepolymer solutions contained 7.5% (m/v) of Phe-PEA or Ala-PEA and 2.5% (m/v) of PEG-DMA or MCS. The photoinitiator, 2-hydroxy-4'-(2-hydroxyethoxy)-2-methylpropiophenone (Irgacure 2959, Sigma-Aldrich) was added last to the solution at a concentration of 0.15% (m/v). The prepolymer solution was then transferred to a 1 mL syringe (Thermo Scientific, Waltham, MA, USA), and photo-crosslinked with long-wavelength ultraviolet light (365 nm) at an intensity of 16 $mW/cm^2$ for 4 min (2 min on each side of the syringe).

**Measurement of gel content and equilibrium water content**. Gel content and equilibrium water content (EWC) were measured in cell-free hydrogels (n = 3). After photo-crosslinking, the

initial mass ($m_i$) of each hydrogel was recorded and the theoretical mass ($m_t$) of polymers involved in crosslinking was calculated as $m_i$ x 0.1 based on 10 m/v % in the formulation. The hydrogels were then swollen in PBS for 24 hr, and the swollen mass ($m_s$) was recorded to determine the EWC. Then, the hydrogels were rinsed three times successively in distilled water for 3 hr to remove remaining non-crosslinked materials and salts from PBS. Following the rinses, the hydrogels were frozen in liquid $N_2$, lyophilized, and their dry masses ($m_d$) were measured. The gel content and EWC were calculated using equations (1) and (2) respectively:

$$\text{Gel content} = \frac{m_d}{m_t} \text{ x } 100\% \qquad (1)$$

$$\text{EWC} = \frac{m_s - m_d}{m_s} \text{ x } 100\% \qquad (2)$$

**Measurement of mass swelling ratio**. After the hydrogels were prepared, their masses ($m_i$) were recorded. The hydrogels were then swollen to equilibrium in PBS at 37 °C for 24 hr, and the swollen mass was recorded ($m_s$). The mass swelling ratio was calculated according to the following equation:

$$\text{Mass swelling ratio} = \frac{m_s - m_i}{m_i} \text{ x } 100\% \qquad (3)$$

**Measurement of the Young's moduli under unconfined compression**. Cylindrical samples with diameters of ~5 mm and heights of ~10 mm (n = 3) were prepared in 1 mL syringes as described above and equilibrated in PBS for 24 hr. Before compression testing, the dimensions of the swollen hydrogels were accurately measured using calipers. Unconfined stress-strain measurements were conducted using a UniVert system (CellScale, Waterloo, ON, Canada), equipped with a 0.5 N load cell. During the measurement, the samples were immersed in a 37 °C

PBS bath, preloaded at 0.01 N at every cycle, and compressed to a total strain of 20% at a rate of 0.6%/s. The nominal stress was calculated by dividing the applied force by the initial cross-sectional area of the sample. The compressive modulus was determined from the slope of the linear region of the stress-strain curve between 10 and 15% strain.

**Human adipose-derived stromal cell isolation and culture**. Adipose tissue was obtained with informed consent from female patients undergoing elective lipo-reduction surgeries at the University Hospital and St. Joseph's Hospital in London, ON, Canada, with Human Research Ethics Board approval from Western University (Protocol #105426). Within 2 hr of extraction, the samples were transported to the lab on ice in sterile phosphate buffer saline (PBS) supplemented with 20 mg/mL bovine serum albumin (BSA). Human ASCs were isolated within 2 hr of procurement using previously published methods [51, 52]. The cells were cultured in proliferation medium comprised of DMEM:Ham's F-12 medium (Wisent Bio Products, Montreal, QC) supplemented with 10% fetal bovine serum (FBS; Wisent Bio Products) and 100 U/mL penicillin and 0.1 mg/mL streptomycin (1% pen-strep; Wisent Bio Products). Fresh proliferation medium was provided every 2-3 days. The cells were passaged at 80% confluence using 0.25% trypsin/0.1% EDTA (Wisent Bio Products) and re-plated in new flasks at 6,000-7,000 cells/$cm^2$. Passage 4 (P4) ASCs were used for all cell encapsulation studies, and each study was repeated with three different donors (N = 3).

**ASC encapsulation and culture within Phe-PEA/Ala-PEA based hydrogels**. The polymer solutions of Phe-PEA or Ala-PEA were prepared as described for the fabrication of the hydrogels. ASCs at P4 were suspended in proliferation medium at a concentration of 1 x $10^7$

cells/mL and combined with the polymer solution for hydrogel encapsulation. The final solution volume contained 80% polymer solution and 20% ASC suspension by volume and was then photo-crosslinked as described above. Immediately after crosslinking, the hydrogels were cut into 25 μL volume disks, each containing ~2.5 x $10^5$ cells, transferred into 12-well inserts (Greiner Bio-one, Germany), and cultured in proliferation medium at 37 °C with 5% $CO_2$. After 24 hr, the hydrogels were transferred into serum-free adipogenic differentiation medium comprised of DMEM:Ham's F-12 nutrient mixture supplemented with 1% pen-strep, 33 μM biotin, 17 μM pantothenate, 10 μg/mL transferrin, 100 nM hydrocortisone, 66 nM insulin, and 1 nM triiodothyronine, with 0.25 mM isobutylmethylxanthine and 1 μg/mL troglitazone included for the first 72 hr [53]. Fresh medium was provided to all samples every 2-3 days.

**Cell viability.** Viability of the encapsulated ASCs in the Phe-PEA and Ala-PEA hydrogels was assessed at 24 hr after encapsulation and at 7 days after the induction of adipogenic differentiation (n = 3 replicate scaffolds/trial, N = 3 trials with different ASC donors) using the LIVE/DEAD® Viability/Cytotoxicity Kit for mammalian cells (Cat. # L-3224; Life Technologies Inc., Burlington, ON, Canada). During preparation, the hydrogels were rinsed twice in PBS before incubation in 1X staining solution for 45 min at 37 °C. Next, the hydrogels were rinsed two times with PBS before imaging using a Zeiss LSM 800 confocal microscope (Zeiss Canada, Toronto, ON, Canada). The complete cross-sectional area of each hydrogel was imaged at 10X magnification and mosaic images were generated using the Zen software (Zeiss Canada) stitching command. A total of 5 layers, separated by 75 μm, were imaged for each hydrogel sample.

Image J analysis software was used to quantify the number of live and dead cells in each layer in order to calculate the average cell viability and density for each group.

**Glycerol-3-phosphate dehydrogenase (GPDH) activity**. Quantitative assessment of ASC adipogenesis was conducted by measuring intracellular GPDH enzyme activity in the Phe-PEA and Ala-PEA hydrogels at 7 days after adipogenic induction (n = 3, N = 3) using a GPDH Enzyme Activity Measurement Kit (Kamiya Biomedical Corporation, Cat. # KT-010, Seattle, WA, USA) following published methods [54, 55]. ASCs cultured on tissue culture polystyrene in 6-well plates in proliferation medium (non-induced) or adipogenic differentiation medium (induced) for 7 days were included as assay controls. To normalize the GPDH activity levels, the total cytosolic protein content for all samples was measured using the Pierce 660 Protein Assay Kit (Thermo Scientific, Waltham, MA, USA) with an albumin standard. Total protein content and GPDH activity were measured using a CLARIOstar® spectrophotometer (BMG Labtech, Ortenberg, Germany).

**BODIPY staining**. Qualitative assessment of ASC adipogenesis was performed using BODIPY® 493/503 staining (Thermo Scientific, Waltham, MA, USA) to visualize intracellular lipid accumulation in the ASCs encapsulated in the Phe-PEA and Ala-PEA hydrogels at 7 days after adipogenic induction (n = 3, N = 3). The BODIPY® was reconstituted in DMSO at 1 mg/mL and diluted in PBS by a factor of 1:500. The hydrogels were rinsed two times in PBS and then incubated in the staining solution at 37 °C for 1 hr. Following incubation, the hydrogels were rinsed twice in PBS before imaging with the Zeiss LSM 800 confocal microscope at 25X magnification.

**Statistical analysis**. Data are reported as the mean ± standard deviation (SD), and the statistical analyses were performed using GraphPad Prism 6 (GraphPad Software, San Diego, CA, USA) by two-way ANOVA with a Tukey's post-hoc test (Figures 3, 5) or t-test (Figure 4g, 6). Differences were considered statistically significant at $p < 0.05$.

## Results and Discussion

**Polymer synthesis and characterization**. The initial objective was to synthesize water-soluble PEAs containing crosslinkable moieties in their backbones to allow for hydrogel formation in aqueous conditions for ASC encapsulation. Monomers **1a**, **1b**, and **1c** (Scheme 1) were synthesized as previously reported from L-phenylalanine or L-alanine and 1,4-butanediol or 1,8-butanediol *via* Fischer esterification [48, 49]. The aim was to compare the effects of the different amino acids and diols on the properties of the resulting PEA hydrogels. However, the monomer composed of L-alanine and 1,4-butanediol could not be prepared in acceptable yield and purity for polymerization. Diamino PEG macromonomer (**2**) (2000 g/mol) was prepared as described in the supporting information *via* tosylation and subsequent amination of PEG diol. The role of macromonomer **2** was to impart water-solubility to the resulting PEAs. Di-*p*-nitrophenyl fumarate (**3**) was synthesized as previously reported [48] to provide crosslinkable moieties along the PEA backbone for hydrogel preparation.

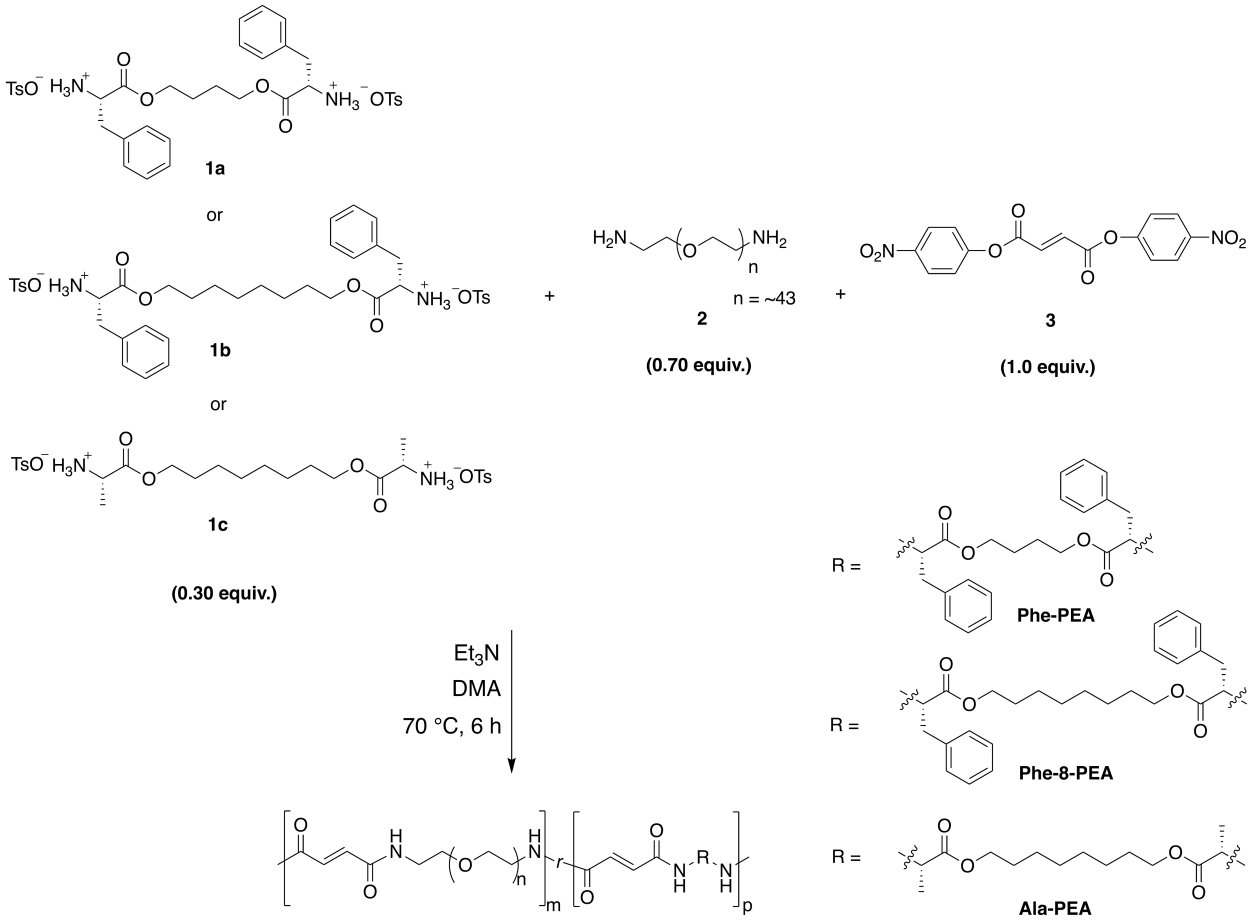


**Scheme 1**. PEA synthesis from different monomer combinations.

The monomers were polymerized under solution polycondensation conditions in DMA at 70 ºC using $NEt_3$ as a base to deprotonate the ammonium salts **1a-c** (Scheme 1). Unlike previous PEA syntheses under similar conditions [49], it was necessary to reduce the polymerization time from 48 hr to 6 hr to avoid undesired crosslinking of the resulting PEAs, which resulted in insoluble gels, presumably due to crosslinking reactions of backbone alkenes from the fumaramide units by Michael-type additions of remaining diamine monomers such as **1** or **2** or due to radical generation upon prolonged heating. Three different ratios of monomers **1**:**2** were examined: 50:50, 40:60 and 30:70. While higher ratios of **1**:**2** led to water-insoluble PEAs, at

30:70 monomers **1**:**2** both Phe-PEA and Ala-PEA were soluble. However, Phe-8-PEA was not water-soluble for any of the prepared ratios.

The molar masses of the polymers were determined by SEC (Table 1). All of the PEAs had $M_n$ values close to 20 kg/mol and $Đ$ values ranging from 2.5 – 3.0. The absence of unreacted macromonomer **2** was confirmed by the absence of a peak in the SEC trace at the location expected for 2000 g/mol PEG (Figure S9). The $Đ$ values were higher than expected for a step-growth polymerization, where they should approach 2.0. This result can likely be attributed to a small degree of crosslinking, which was not a concern as the PEAs were designed to be incorporated in subsequent steps into a network.

**Table 1.** Molar mass data for the PEAs, as measured by SEC.

| **Polymer** | $M_n$ **(kg/mol)** | $M_w$ **(kg/mol)** | $Đ$ |
|---|---|---|---|
| Phe-PEA | 19.9 | 49.2 | 2.46 |
| Phe-8-PEA | 20.1 | 56.6 | 2.81 |
| Ala-PEA | 18.9 | 56.1 | 2.96 |

$^1$H NMR and FT-IR spectroscopic analyses were consistent with the structures of the proposed polymers. $^1$H NMR spectra had peaks at ~8.8 and 8.5 ppm corresponding to the amide -N*H*- protons adjacent to monomers **1** and macromonomer **2** respectively (Figure 1, S5-S7). The spectra also had peaks at ~6.8 ppm corresponding to the =C*H* fumaramide units along the backbone and peaks at 3.5 ppm corresponding to PEG. The spectrum of Phe-PEA was differentiated from that of Ala-PEA by the presence of peaks corresponding to the pendent phenyl groups of phenylalanine from 7.3 to 7.2 ppm, and the peaks from 3.1 – 2.9 ppm due to the

-C$H_2$- moieties adjacent to the phenyl groups (Figure 1a). In contrast, Ala-PEA had peaks at ~1.3 ppm corresponding to the backbone octyl chain and pendent methyl groups on alanine (Figure 1b). Overall, the integrations of the peaks corresponded closely to the feed molar ratios of monomer **1:2:3** at 0.3:0.7:1.0 (Figures S5-S7). The FT-IR spectra were also consistent with the successful synthesis of PEAs with characteristic peaks corresponding to the amide N-H stretch at 3300 $cm^{-1}$, the ester C=O stretch at 1740 $cm^{-1}$, the amide C=O stretch at 1640 $cm^{-1}$, and the amide N-H bend at 1550 $cm^{-1}$ (Figure S8).

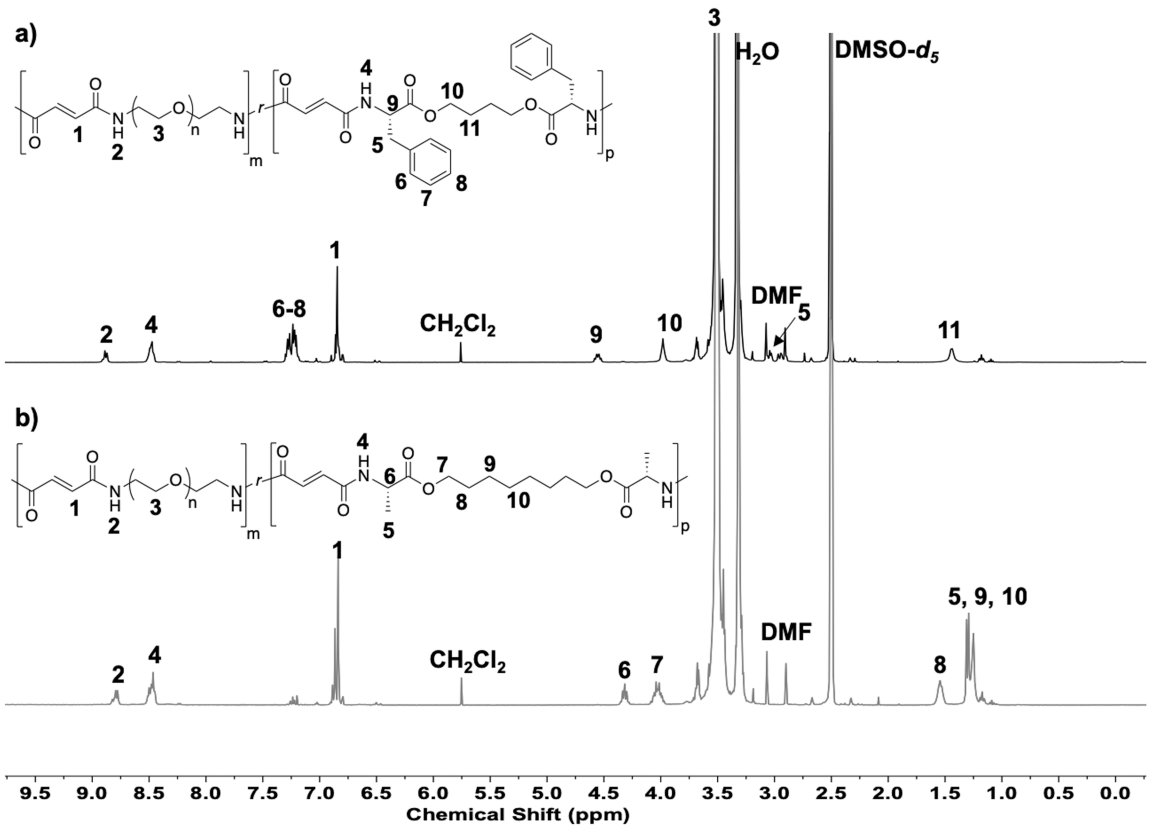


**Figure 1.** $^1$H NMR spectra of a) Phe-PEA and b) Ala-PEA in DMSO-$d_6$ (400 MHz).

**Fabrication and characterization of hydrogels.** After the successful synthesis of the water-soluble PEAs Phe-PEA and Ala-PEA with backbone alkenes for crosslinking, their gelation was

investigated. Irgacure 2959 was used as a photoinitiator at a concentration of 0.15% (m/v). In addition to formulations incorporating only the PEAs (10 % m/v) and initiator, formulations incorporating PEG-DMA or MCS at 2.5% (m/v) (Figure 2) in addition to PEA at 7.5% (w/v) were also investigated to tune the hydrogel properties. PEG-DMA was selected because PEG tends to be well tolerated *in vivo* and has been extensively used for hydrogel formation [10, 56]. MCS was selected as it has previously been shown to provide a microenvironment that supports the viability and adipogenic differentiation of encapsulated human ASCs [54, 55], and increased production of soluble and cell-associated chondroitin 4-sulphate proteoglycans has also been linked to adipogenesis in the murine 3T3-L1 preadipocyte cell line [57]. Crosslinking was performed in syringes and was induced by irradiation with 365 nm light for 4 min (2 min per side of syringe). These conditions were previously found to be well tolerated by ASCs when encapsulated into MCS-based hydrogels [58].

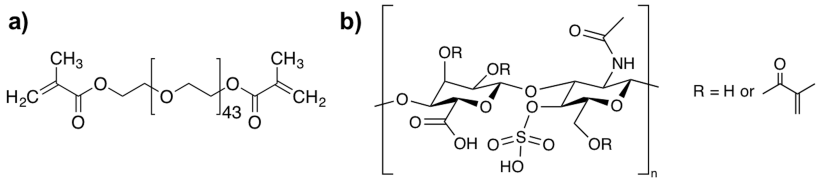


**Figure 2.** Chemical structures of a) PEG-DMA and b) MCS.

To understand the effects of the different hydrogel compositions on their properties, all of the hydrogels were characterized by the measurement of their gel content, EWC and mass swelling ratio. Gel content is the mass percentage of material successfully incorporated into the network, while EWC represents the swelling degree of the crosslinked network with water relative to the dry weight of gel. For gel content, there was a common trend that all Phe-PEA-based systems had a higher gel content than the Ala-PEA-based systems (Figure 3a). However,

the difference was only statistically significant for the systems with PEG-DMA incorporated. The incorporation of PEG-DMA or MCS generally decreased the gel content relative to that of the pure PEA, but again the difference was only statistically significant when comparing pure Ala-PEA to Ala-PEA + PEG-DMA. The results suggest that the additives disrupted the crosslinking to a small extent, perhaps due to phase separation with the PEA or due to poor compatibility of the methacrylates with the fumaramides in the polymerization reaction. There were no significant differences in the EWC across the examined hydrogels. Although the differences were not statistically significant, the Ala-PEA hydrogels tended to swell more than the Phe-PEA hydrogels. Higher swelling may be attributed to the trend towards lower gel content for the Ala-PEA hydrogels, as lower gel content would suggest a lower density of crosslinks in the network. However, it could also relate to the relative hydrophilicities of the PEAs. Although the alanine-based monomer **1c** has a longer aliphatic diol chain than the phenylalanine monomer **1a**, the methyl side chains on alanine are much less hydrophobic than the phenyl side chains of phenylalanine. Overall, the hydrogels with PEG-DMA and MCS incorporated tended to swell more than those prepared from pure PEAs. This result may relate to their lower gel content, and also to the presence of charges on MCS, which results in an influx of water through osmosis.

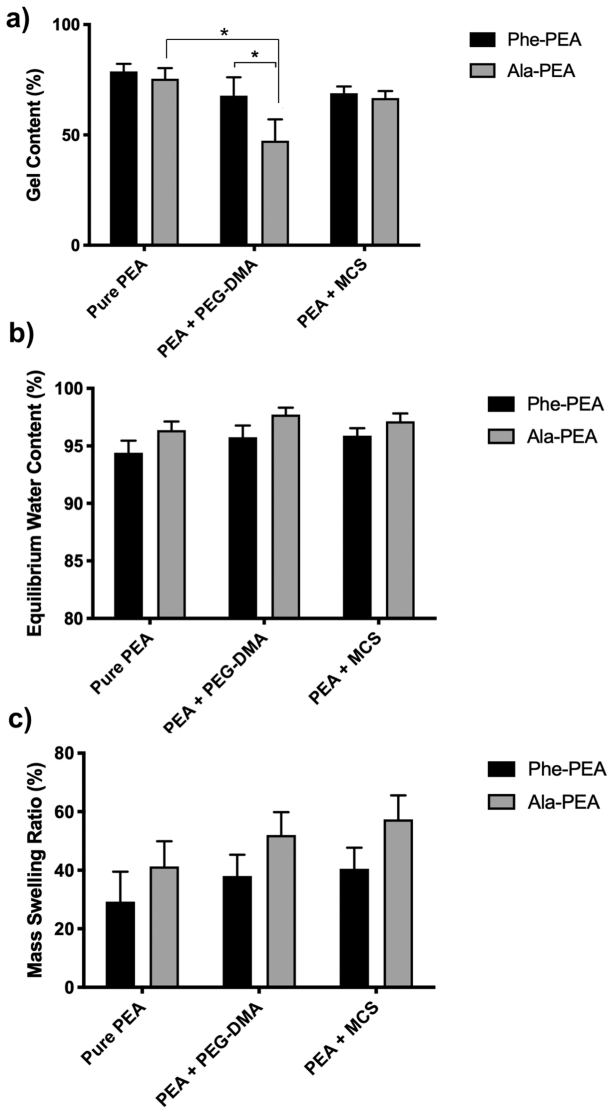


**Figure 3.** a) Gel content of the hydrogels; b) Equilibrium water content of the hydrogels; c) Mass swelling ratio of the hydrogels. The experiments were performed in triplicate and the data are presented as the mean, with error bars corresponding to the SD. Data were analyzed by two-way ANOVA with a Tukey's post-hoc comparison of the means ($p < 0.05$). *denotes a statistically significant difference between groups.

The Young's moduli of selected hydrogels were evaluated under unconfined compression. These efforts focused on hydrogels composed of the pure PEAs as hybrid hydrogels containing

PEG-DMA or MCS were very brittle and tended to fracture (Figure 4a-f), making compression testing impossible and prohibiting their inclusion in the cell encapsulation studies. Similar to their lower gel contents, the poor mechanical properties of the hydrogels containing PEG-DMA or MCS can likely be attributed to the disruption of crosslinking due to polymer phase separation or incompatibilities between crosslinking moieties.

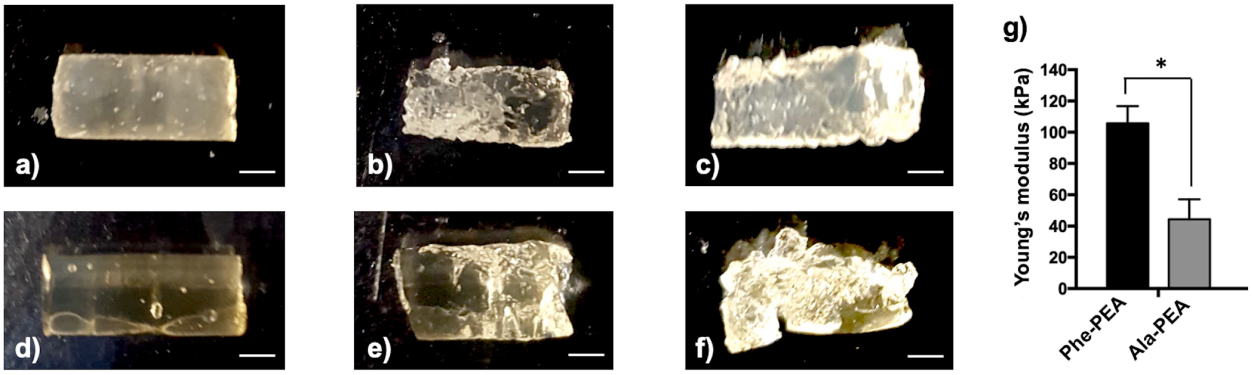


**Figure 4.** Representative images of the hydrogels after removal from the syringe mold: a) Phe-PEA, b) Phe-PEA + PEG-DMA, c) Phe-PEA + MCS, d) Ala-PEA, e) Ala-PEA + PEG-DMA and f) Ala-PEA + MCS. Scale bar: 5 mm. Hydrogels prepared with PEG-DMA and MCS tended to fracture. g) Comparison of the Young's moduli of Phe-PEA and Ala-PEA measured under unconfined compression. The experiments were performed in triplicate and the data are presented as the mean, with error bars corresponding to the SD. Data were analyzed by a t-test ($p < 0.05$). *denotes a statistically significant difference between groups.

For the pure PEAs, Phe-PEA had a modulus of 106 ± 11 kPa and Ala-PEA had a modulus of 44 ± 13 kPa. The higher moduli for the Phe-PEA hydrogels may result from their trend towards lower EWC and swelling relative to the Ala-PEA systems, as this would result in a higher density of polymer in the network, leading to higher stiffness. Hydrophobic interactions between the phenyl groups in Phe-PEA, may also contribute to higher stiffness. The moduli of

both hydrogels were higher than that of adipose tissue, which is ~ 2-4 kPa, but in the range of other soft tissues such as muscle, bladder, and cornea [59] and similar to previous chitosan- and chondroitin sulfate-based hydrogels that have been shown to support the viability and adipogenic differentiation of ASCs [54].

**Cell viability.** To assess the capacity of the hydrogel scaffolds to support ASCs during encapsulation and adipogenic induction, the viability of ASCs encapsulated in the Phe-PEA and Ala-PEA hydrogels was assessed at 24 hr post-encapsulation, as well as at 7 days after adipogenic induction, through LIVE/DEAD® imaging analysis by confocal microscopy (Figure 5). Visualization of the cell distribution across the complete cross-section of the hydrogels revealed that there was a more homogenous distribution of ASCs in the Ala-PEA hydrogels, which was particularly evident at 24 hr (Figure 5a). Notably, the Phe-PEA polymer solution was more viscous, which made mixing to combine it with the ASC suspension more challenging and likely resulted in the observed regions that were devoid of cells.

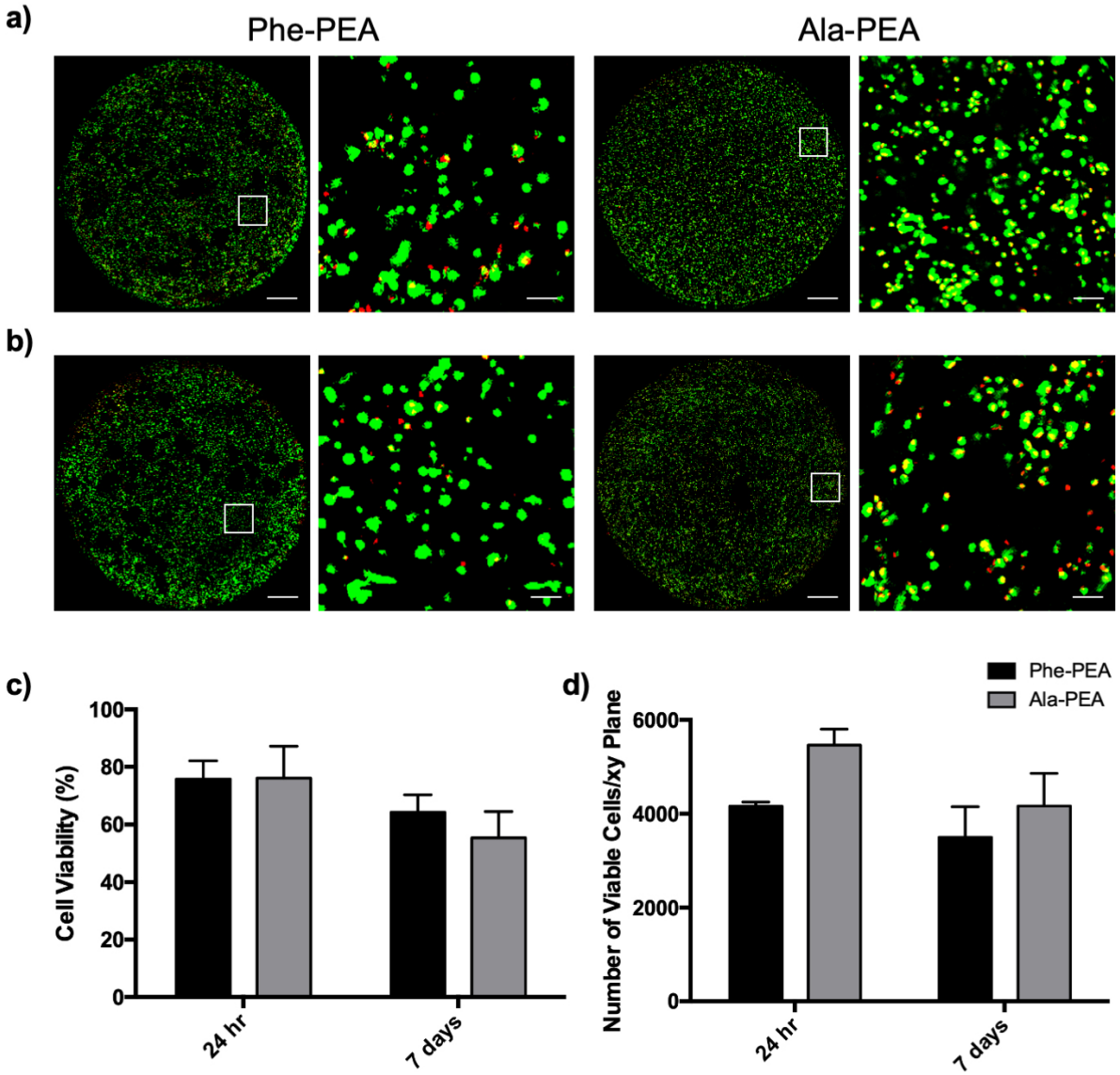


**Figure 5.** Viability analysis of ASCs encapsulated in the Phe-PEA and Ala-PEA hydrogels. Representative images of the encapsulated ASCs at a) 24 hr after encapsulation and b) 7 days after adipogenic induction displaying the distribution of live (green; calcein-AM$^{+}$) and dead (red; ethidium homodimer-1$^{+}$) cells. Higher magnification images of the boxed regions in each complete hydrogel cross-section (scale bar: 500 μm) are shown on the right (scale bar: 50 μm). c) Percent viability and d) average number of viable ASCs per xy plane in the Phe-PEA and Ala-PEA hydrogels. Data are presented as the mean with error bars corresponding to the standard

deviations (n = 3 hydrogel replicates/trial, N = 3 trials with different ASC donors). Data were analyzed by two-way ANOVA with a Tukey's post-hoc comparison of the means. No significant differences were observed between any of the groups.

Quantification of the staining at 24 hr post-encapsulation indicated that the ASC viability in both the Phe-PEA and Ala-PEA hydrogels was > 75%, with no significant differences observed between the systems (Figure 5c). These findings are similar to previous levels observed with human ASCs encapsulated into MCS or methacrylated glycol chitosan (MGC) hydrogels via light-initiated crosslinking [54]. Overall, the viability results at 24 hr support that the encapsulation process was well-tolerated by the human ASCs. While not statistically significant, lower ASC viability was observed after 7 days of culture in adipogenic differentiation medium for both hydrogel groups. Again, these results are consistent with previous levels reported for the ASCs encapsulated in the MCS and MGC hydrogels, where a decline in viability was observed after 14 days of culture in adipogenic differentiation medium [54]. While favorable for inducing growth arrest in order to stimulate ASC adipogenesis, the lack of serum within the adipogenic differentiation medium may have contributed to the trend for declining viability over time in culture. To try to mitigate these effects, in the future it would be interesting to explore the incorporation of ECM components, such as decellularized adipose tissue (DAT) particles, which were previously shown to enhance the long-term viability and adipogenic differentiation of ASCs within the MCS and MGC hydrogels [54]. Similar to the viability results, there were no significant differences observed in the viable cell density per plane for either of the hydrogel groups at both time points studied (Figure 5d), indicating that differences in ASC density were

not a confounding factor in comparing the levels of adipogenic differentiation between the two systems [55].

**Assessment of adipogenesis.** The capacity of the hydrogels to support the adipogenic differentiation of the encapsulated ASCs for potential adipose tissue engineering applications was also assessed. Quantification of GPDH enzyme activity, which is upregulated during ASC adipogenesis, indicated that there were no significant differences between the Phe-PEA and Ala-PEA groups at 7 days post-induction of differentiation, with both groups showing enhanced levels compared to the non-induced tissue culture controls (Figure 6a). The GPDH activity levels observed were similar to those previously reported for the human ASCs encapsulated in the MCS and MGC hydrogels at 7 days [54]. The enhanced GPDH activity in the induced tissue culture controls relative to the hydrogel groups may be related to the high levels of cell-cell contact achieved in the high-density 2-D cultures as compared to the distribution of single cells that was observed within the hydrogels [55, 60]. Consistent with the GPDH results, BODIPY staining revealed a qualitatively-similar and abundant number of lipid-loaded cells in both the Phe-PEA and Ala-PEA hydrogels (Figure 6b), confirming that both systems were supportive of ASC adipogenesis. In the future, it would be worthwhile to explore the effects of increasing the cell density within the hydrogels, as well as extending the studies to longer timepoints, to elucidate whether there may be subtle differences in the capacity of the two PEA formulations to promote the adipogenic differentiation of the human ASCs that could be detected under varying culture conditions.

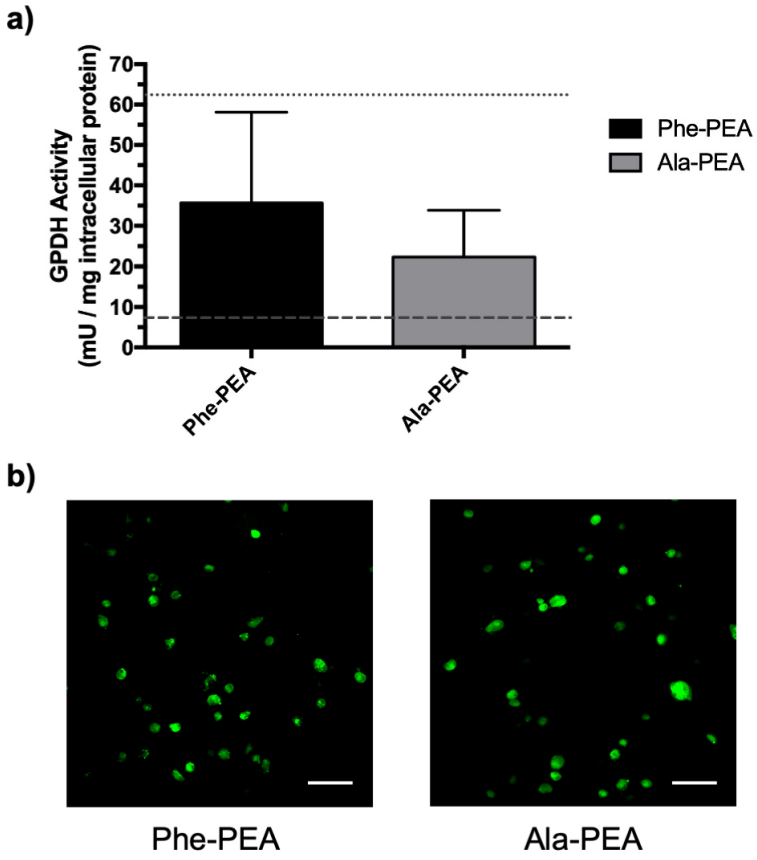


**Figure 6.** *In vitro* analysis of ASC adipogenesis within the hydrogels at 7 days post-induction of differentiation. a) GPDH enzyme activity for ASCs encapsulated in either Phe-PEA or Ala-PEA hydrogels. Data are presented as the mean with error bars corresponding to the standard deviations (n = 3 hydrogel replicates/trial, N = 3 trials with different ASC donors). Dotted and dashed lines represent the mean values for the induced (cultured in adipogenic differentiation medium) and non-induced (cultured in proliferation medium) tissue culture control groups respectively. The hydrogel groups were compared with a t-test and no significant differences were observed. b) Representative images of BODIPY-stained (green) ASCs encapsulated in the Phe-PEA and Ala-PEA hydrogels showing qualitatively similar numbers of differentiating ASCs containing intracellular lipid droplets after 7 days of culture in adipogenic differentiation medium. Scale bar: 50 μm

## Conclusions

New water-soluble PEAs with crosslinkable moieties in their backbones were successfully synthesized from a phenylalanine-based monomer, alanine-based monomer, *p*-nitrophenyl fumarate and a PEG diamine. The PEAs were only water soluble when a 70:30 ratio of PEG:amino acid monomer was used and for Phe-PEA and Ala-PEA, but not Phe-8-PEA. Using 365 nm light and a photoinitiator, hydrogels were prepared from the pure PEAs (10% w/v) and from the PEAs (7.5% w/v) with either PEG-DMA (2.5% w/v) or MCS (2.5% w/v). The Phe-PEA hydrogels tended to exhibit higher gel content, lower EWC and less swelling than the Ala-PEA hydrogels, though the differences were small and not statistically significant in many cases. The incorporation of PEG-DMA or MCS tended to decrease the gel content, increase the EWC, increase the swelling, and made the hydrogels brittle. Hydrogels composed of pure Phe-PEA and Ala-PEA had Young's moduli of 106 and 44 kPa respectively. Human ASCs were successfully encapsulated within the Phe-PEA and Ala-PEA hydrogels via light-initiated crosslinking, with viabilities higher than 75% at 24 hr. While there was a trend towards declining viability over time in culture, the Phe-PEA and Ala-PEA hydrogels were shown to similarly support the adipogenic differentiation of the encapsulated ASCs, with an abundant number of lipid-loaded cells observed after only 7 days of culture in adipogenic differentiation medium. Overall, the findings support the further investigation of these novel water-soluble PEAs as an ASC delivery platform for applications in adipose tissue regeneration.

## Acknowledgements

This research was funded by the Natural Sciences and Engineering Research Council of Canada (NSERC) CREATE Training Grant (2015-465675), NSERC Discovery Grant (2016-04636), the

Western Bone and Joint Institute (Collaborative Specialization in Musculoskeletal Health Research Fellowship to N. L.) and the Canadian Institutes for Health Research (Operating Grant 119394). N. L. thanks Dr. Arthi Shridhar, Nadia Sharma, and Dr. Pascal Morissette Martin for their technical assistance with cell culture, microscopy, and data analysis.

**Supporting information**

Additional synthesis procedures, NMR spectra, FT-IR spectra, SEC traces

**Data availability**

The processed data required to reproduce these findings are available to download from [insert linking to the supporting information]. Raw data is available upon request.

**References**

[1] H. Wang, S.C. Heilshorn, Adaptable hydrogel networks with reversible linkages for tissue engineering, Adv. Mater. 27 (2015) 3717-3736.

[2] A. Khademhosseini, R. Langer, A decade of progress in tissue engineering, Nat. Protoc. 11 (2016) 1775-1781.

[3] T. Delair, In situ forming polysaccharide-based 3D-hydrogels for cell delivery in regenerative medicine, Carbohydr. Polym. 87 (2012) 1013-1019.

[4] C. Dong, Y. Lv, Application of collagen scaffold in tissue engineering: Recent advances and new perspectives, Polymers 8 (2016) 42, doi:10.3390/polym8020042.

[5] A.C. Hernandez-Gonzalez, L. Tellez-Jurado, L.M. Rodriguez-Lorenzo, Alginate hydrogels for bone tissue engineering, from injectables to bioprinting: A review, Carbohydr. Polym. 229 (2019) 115514.

[6] P.K. Dutta, Chitin and chitosan for regenerative medicine, Springer, Berlin, Germany, 2016.

[7] C.B. Highley, G.D. Prestwich, J.A. Burdick, Recent advances in hyaluronic acid hydrogels for biomedical applications, Curr. Opin. Biotech. 40 (2016) 35-40.

[8] J. Yang, M. Shen, H. Wen, Y. Luo, R. Huang, L. Rong, J. Xie, Recent advance in delivery system and tissue engineering applications of chondroitin sulfate, Carbohydr. Polym. 230 (2019) 115650.

[9] S.-B. Park, E. Lih, E.-S. Park, Y.K. Joung, D.K. Han, Biopolymer-based functional composites for medical applications, Prog. Polym. Sci. 68 (2017) 77-105.

[10] E. Bakaic, N.M.B. Smeets, T. Hoare, Injectable hydrogels based on poly(ethylene glycol) and derivatives as functional biomaterials, RSC Adv. 5 (2015) 35469-35486.

[11] L.J. MacDougall, K. Anseth, Bioerodible hydrogels based on photopolymerized poly(ethylene glycol)-co-poly(alpha-hydroxy acid) diacrylate macromers, Macromolecules 53 (2020) 2295-2298.

[12] A. Basu, K.R. Kunduru, S. Doppalapudi, A. Domb, W. Khan, Poly(lactic acid) based hydrogels, Adv. Drug Delivery Rev. 107 (2016) 192-205.

[13] E. Armelin, S. Lanzalaco, Poly(N-isopropylacrylamide) and copolymers: A review on recent progresses in biomedical applications, Gels 3 (2017) 36/1-36/31.

[14] M. Winnacker, B. Rieger, Poly(ester amide)s: Recent insights into synthesis, stability and biomedical applications, Polym. Chem. 7 (2016) 7039-7046.

[15] A.C. Fonseca, M.H. Gil, P.N. Simoes, Biodegradable poly(ester amide)s - a remarkable opportunity for the biomedical area: Review on the synthesis, characterization and applications, Prog. Polym. Sci. 39 (2014) 1291-1311.

[16] K. Ghosal, M.S. Latha, S. Thomas, Poly(ester amides) (PEAs) – scaffold for tissue engineering applications, Eur. Polym. J. 60 (2014) 58-68.

[17] S.K. Murase, J. Puiggali, Poly(ester amide)s: Recent developments on synthesis and applications, in: S. Kumbar, C. Laurencin, M. Deng (Eds.), Natural and synthetic biomedical polymers, Elsevier, Burlington, MA, 2014, pp. 145-166.

[18] A. Díaz, R. Katsarava, J. Puiggalí, Synthesis, properties and applications of biodegradable polymers derived from diols and dicarboxylic acids: From polyesters to poly(ester amide)s, Int. J. Mol. Sci. 15 (2014) 7064-7123.

[19] I.J. Villamagna, T.N. Gordon, M.B. Hurtig, F. Beier, E.R. Gillies, Poly(ester amide) particles for controlled delivery of celecoxib, J. Biomed. Mater. Res., Part A 107 (2019) 1235-1243.

[20] I.J. Villamagna, D.M. McRae, A. Borecki, X. Mei, F. Lagugné-Labarthet, F. Beier, E.R. Gillies, GSK3787-loaded poly(ester amide) particles for intra-articular drug delivery, Polymers 12 (2020) 736.

[21] M. Janssen, U.T. Timur, N. Woike, T.J. Welting, G. Draaisma, M. Gijbels, L.W. van Rhijn, G. Mihov, J. Thies, P.J. Emans, Celecoxib-loaded PEA microspheres as an auto regulatory drug-delivery system after intra-articular injection, J. Controlled Release 244 (2016) 30-40.

[22] D.K. Knight, R. Stutchbury, D. Imruck, C. Halfpap, S. Lin, U. Langbein, E.R. Gillies, S. Mittler, K. Mequanint, Focal contact formation of vascular smooth muscle cells on langmuir-blodgett and solvent-cast films of biodegradable poly(ester amide)s, ACS Appl. Mater. Interfaces 4 (2012) 1303-1312.

[23] M. Deng, J. Wu, C.A. Reinhart-King, C.C. Chu, Synthesis and characterization of biodegradable poly(ester amide)s with pendant amine functional groups and in vitro cellular response, Biomacromolecules 10 (2009) 3037-3047.

[24] S.H. Lee, I. Szinai, K. Carpenter, R. Katsarava, G. Jokhadze, C.C. Chu, Y. Huang, E. Verbeken, O. Bramwel, I. De Scheerder, M.K. Hong, In vivo biocompatibility evaluation of stents coated with a new biodegradable elastomeric and functional polymer, Coronary Artery Dis. 13 (2002) 237-241.

[25] K.M. DeFife, K. Grako, G. Cruz-Aranda, S. Price, R. Chantung, K. MacPherson, R. Khoshabeh, S. Gopalan, A.G. Turnell, Poly(ester amide) copolymers promote blood and tissue compatibility, J. Biomater. Sci. Polym. Ed. 20 (2009) 1495-1511.

[26] J. Liu, X.L. Liu, T.F. Xi, C.C. Chu, A novel pseudo-protein-based biodegradable coating for magnesium substrates: In vitro corrosion phenomena and cytocompatibility, J. Mater. Chem. B 3 (2015) 878-893.

[27] L. Li, C.C. Chu, Nitroxyl radical incorporated electrospun biodegradable poly(ester amide) nanofiber membranes, J. Biomater. Sci., Polym. Ed. 20 (2009) 341-361.

[28] S.S. Said, J.G. Pickering, K. Mequanint, Controlled delivery of fibroblast growth factor-9 from biodegradable poly(ester amide) fibers for building functional neovasculature, Pharm. Res. 31 (2014) 3335-3347.

[29] S.K. Murase, L.J. del Valle, S. Kobauri, R. Katsarava, J. Puiggali, Electrospun fibrous mats from a l-phenylalanine based poly(ester amide): Drug delivery and accelerated degradation by loading enzymes, Polym. Deg. Stabil. 119 (2015) 275-287.

[30] D.K. Knight, E.R. Gillies, K. Mequanint, Biomimetic l-aspartic acid-derived functional poly(ester amide)s for vascular tissue engineering, Acta Biomater. 10 (2014) 3484-3496.

[31] L.J. del Valle, D. Roca, L. Franco, J. Puiggali, A. Rodriguez-Galan, Preparation and release study of ibuprofen-loaded porous matrices of a biodegradable poly(ester amide) derived from l-alanine units, J. Appl. Polym. Sci. 122 (2011) 1953-1967.

[32] K. Cao, D.S. Flegg, S. Lin, F. Lagugné-Labarthet, K. Mequanint, E.R. Gillies, Fabrication and in situ cross-linking of carboxylic-acid-functionalized poly(ester amide) scaffolds for tissue engineering, ACS Appl. Polym. Mater. 1 (2019) 2360-2369.

[33] P. Karimi, A.S. Rizkalla, K. Mequanint, Versatile biodegradable poly(ester amide)s derived from alpha-amino acids for vascular tissue engineering, Materials 3 (2010) 2346-2368.

[34] G.J. Zilinskas, A. Soleimani, E.R. Gillies, Poly(ester amide)-poly(ethylene oxide) graft copolymers: Towards micellar drug delivery vehicles, Int. J. Polym. Sci. 2012 (2012) 564348.

[35] R. Soleimani, A. Borecki, E.R. Gillies, Photodegradable poly(ester amide)s for indirect light-triggered release of paclitaxel, Polym. Chem. 5 (2014) 7062-7071.

[36] A. Soleimani, M.M. Abd Rabo Moustafa, A. Borecki, E.R. Gillies, A comparison of covalent and noncovalent strategies for paclitaxel release using poly(ester amide) graft copolymer micelles., Can. J. Chem. 93 (2015) 399-405.

[37] J. Wu, D. Wu, A. Mutschler, C.-C. Chu, Synthesis and characterization of ionic charged water soluble arginine-based poly(ester amide), J. Mater. Sci. Mater. Med. 22 (2011) 469-479.

[38] J. Wu, D. Wu, A. Mutschler, C.-C. Chu, Cationic hybrid hydrogels from amino-acid-based poly(ester amide): Fabrication, characterization, and biological properties, Adv. Funct. Mater. 22 (2012) 3815-3823.

[39] Q. Wu, J. Wu, C.C. Chu, A novel family of biodegradable hybrid hydrogels from arginine-based poly(ester amide) and hyaluronic acid precursors, Soft Matter 9 (2013) 3965-3975.

[40] M. He, A. Potuck, Y. Zhang, C.C. Chu, Arginine-based polyester amide/polysaccharide hydrogels and their biological response, Acta Biomater. 10 (2014) 2482-2494.

[41] Z. Gu, J. Wu, K. Huang, Black phosphorus hydrogel scaffolds enhance bone regeneration via a sustained supply of calcium-free phosphorus, ACS Appl. Mater. Interfaces 11 (2019) 2908-2916.

[42] X. Pang, J. Wu, C.C. Chu, X. Chen, Development of an arginine-based cationic hydrogel platform: Synthesis, characterization and biomedical applications, Acta Biomater. 10 (2014) 3098-3107.

[43] S.K. Samal, M. Dash, S. Van Vlierberghe, D.L. Kaplan, E. Chiellini, C. Van Blitterswijk, L. Moroni, P. Dubruel, Cationic polymers and their therapeutic potential, Chem. Soc. Rev. 41 (2012) 7147-7194.

[44] A.D. Robison, S. Sun, M.F. Poyton, G.A. Johnson, J.P. Pellois, P. Jungwirth, M. Vazdar, P.S. Cremer, Polyarginine interacts more strongly and cooperatively than polylysine with phospholipid bilayers, J. Phys. Chem. B 120 (2016) 9287-9296.

[45] P.A. Zuk, M. Zhu, H. Mizuno, J. Huang, J.W. Futrell, A.J. Katz, P. Benhaim, H.P. Lorenz, M.H. Hedrick, Multilineage cells from human adipose tissue: Implications for cell-based therapies, Tissue Eng. 7 (2001) 211-228.

[46] N.A. O'Halloran, E.B. Dolan, M.J. Kerin, A.J. Lowery, G.P. Duffy, Hydrogels in adipose tissue engineering—potential application in post-mastectomy breast regeneration, Tissue Eng. Regen. Med. 12 (2018) 2234-2247.

[47] C.M. Mahoney, C. Imbarlina, C.C. Yates, K.G. Marra, Current therapeutic strategies for adipose tissue defects/repair using engineered biomaterials and biomolecule formulations, Front. Pharmacol. 9 (2018) Article 507.

[48] K. Guo, C.C. Chu, E. Chkhaidze, R. Katsarava, Synthesis and characterization of novel biodegradable unsaturated poly(ester amide)s, J. Polym. Sci., Part A: Polym. Chem. 43 (2005) 1463-1477.

[49] K.M. Atkins, D. Lopez, D.K. Knight, K. Mequanint, E.R. Gillies, A versatile approach for the syntheses of poly(ester amide)s with pendant functional groups, J. Polym. Sci. Part A: Polym. Chem. 47 (2009) 3757-3772.

[50] A. Shridhar, E. Gillies, B.G. Amsden, L.E. Flynn, Composite bioscaffolds incorporating decellularized ecm as a cell-instructive component within hydrogels as in vitro models and cell delivery systems, Methods Mol. Biol. 1577 (2017) 183-208.

[51] L.E. Flynn, J.L. Semple, K.A. Woodhouse, Decellularized placental matrices for adipose tissue engineering, J. Biomed. Mater. Res., Part A 79 (2006) 359-369.

[52] L.E. Flynn, The use of decellularized adipose tissue to provide an inductive microenvironment for the adipogenic differentiation of human adipose-derived stem cells, Biomaterials 31 (2010) 4715-4724.

[53] G. Ailhaud, H. Hauner, T. Skurk, M. Wabitsch, Cultures of human adipose precursor cells, Methods Mol. Biol. 155 (2001) 239-247.

[54] H.K. Cheung, T.T.Y. Han, D.M. Marecak, J.F. Watkins, B.G. Amsden, L.E. Flynn, Composite hydrogel scaffolds incorporating decellularized adipose tissue for soft tissue engineering with adipose-derived stem cells, Biomaterials 35 (2014) 1914-1923.

[55] C.F.C. Brown, J. Yan, T.T.Y. Han, D.M. Marecak, B.G. Amsden, L.E. Flynn, Effect of decellularized adipose tissue particle size and cell density on adipose-derived stem cell proliferation and adipogenic differentiation in composite methacrylated chondroitin sulphate hydrogels, Biomed. Mater. 10 (2015) 045010.

[56] P.M. Pfister, M. Wendkandt, P. Neuenschwander, U.W. Suter, Surface-textured PEG-based hydrogels with adjustable elasticity: Synthesis and characterization, Biomaterials 28 (2007) 567-575.

[57] J.C. Calvo, D. Rodbard, A. Katki, S. Chernick, M. Yanagishita, Differentiation of 3T3-L1 preadipocytes with 3-isobutyl-1-methylxanthine and dexamethasone stimulates cell-associated and soluble chondroitin 4-sulfate proteoglycans, J. Biol. Chem. 266 (1991) 11237-11244.

[58] A. Shridhar, B.G. Amsden, E.R. Gillies, L.E. Flynn, Investigating the effects of tissue-specific extracellular matrix on the adipogenic and osteogenic differentiation of human adipose-derived stromal cells within composite hydrogel scaffolds, Front. Bioeng. Biotech. 7 (2019) Article 402.

[59] C.F. Guimarães, L. Gasperini, A.P. Marques, R.L. Reis, The stiffness of living tissues and its implications for tissue engineering, Nat. Rev. Mater. 5 (2020) 351-370.

[60] M. Wiesner, O. Berberich, C. Hoefner, T. Blunk, P. Bauer-Kreisel, Gap junctional intercellular communication in adipose-derived stromal/stem cells is cell density-dependent and positively impacts adipogenic differentiation, J. Cell. Physiol. 233 (2018) 3315-3329.